OPEN ACCESS

ARTICLE

Elevating gas turbine system efficiency by integration with super-high-temperature solid oxide fuel cells

Xin Gu,[1] Yuqing Wang,[2,*] Yixiang Shi,[1,3,*] and Ningsheng Cai[1]

*Correspondence: wangyq@bit.edu.cn(Y. W.); shyx@tsinghua.edu.cn(Y. S.)

Received: November 28, 2024; Accepted: May 12, 2025; Published Online: June 4, 2025; https://doi.org/10.59717/j.xinn-energy.2025.100096

GRAPHICAL ABSTRACT

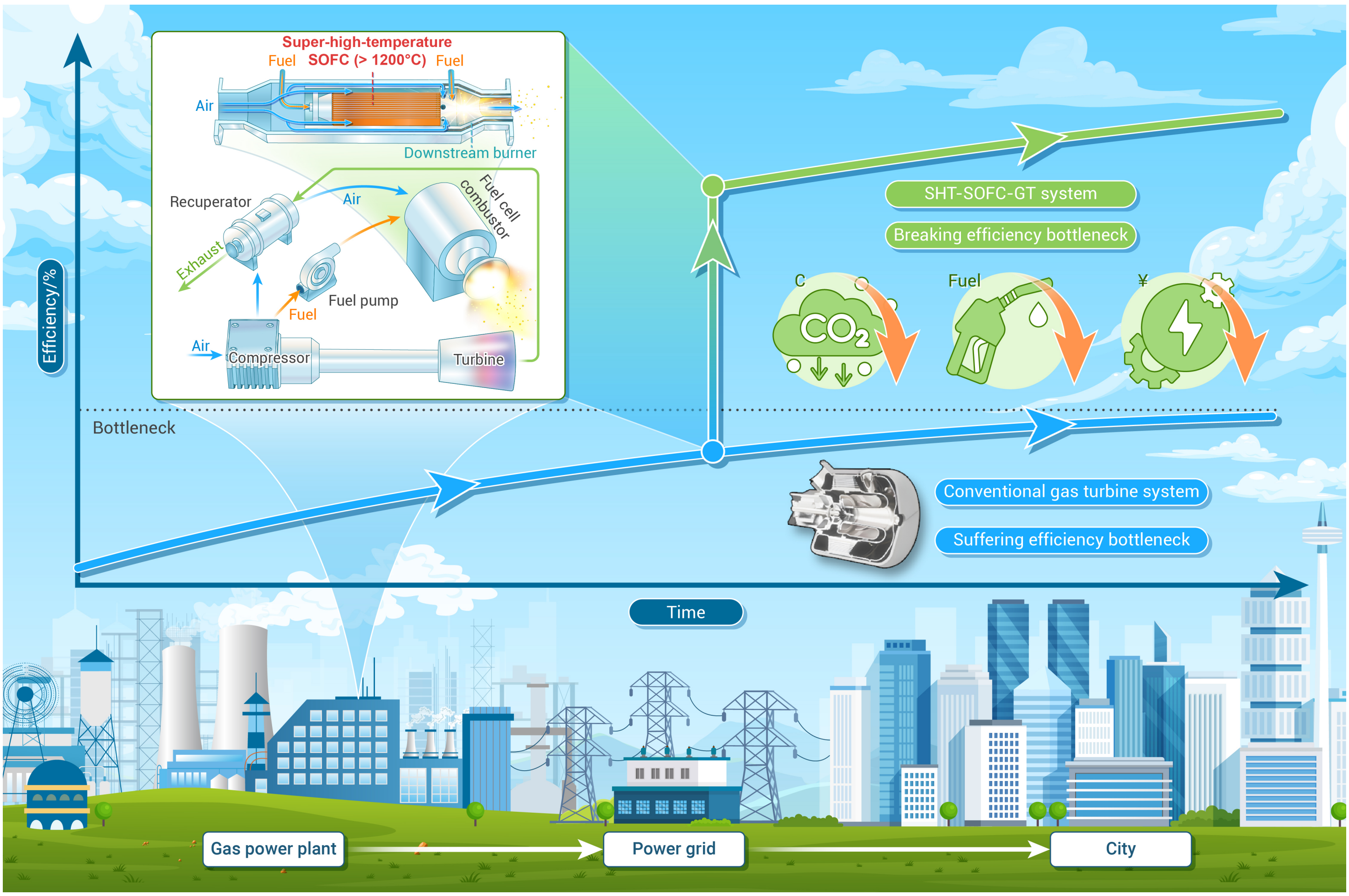

PUBLIC SUMMARY

- A tubular super-high-temperature solid oxide fuel cell (SHT-SOFC) achieved a peak power of 4.67 W at 1200°C .
- The SHT-SOFC can achieve well temperature match with commercial hundred-MW-class gas turbine (GT).
- A super-high efficiency of 80.31% can be expected when SOFC temperature is further elevated to 1300°C.
- Extending the SHT-SOFCs lifespan is crucial for improving the techno-economic performance.

Elevating gas turbine system efficiency by integration with super-high-temperature solid oxide fuel cells

Xin Gu,[1] Yuqing Wang,[2,*] Yixiang Shi,[1,3,*] and Ningsheng Cai[1]

[1]Key Laboratory for Thermal Science and Power Engineering of Ministry of Education, Department of Energy and Power Engineering, Tsinghua University, Beijing 100084, China

[2]National Key Laboratory on Electromechanical Dynamic Control, Beijing Institute of Technology, Beijing 100081, China

[3]Shanxi Research Institute for Clean Energy, Tsinghua University, Taiyuan 030032, China

*Correspondence: wangyq@bit.edu.cn(Y. W.); shyx@tsinghua.edu.cn(Y. S.)

Received: November 28, 2024; Accepted: May 12, 2025; Published Online: June 4, 2025; https://doi.org/10.59717/j.xinn-energy.2025.100096

Citation: Gu X., Wang Y., Shi Y., et al. (2025). Elevating gas turbine system efficiency by integration with super-high-temperature solid oxide fuel cells. *The Innovation Energy* **2**:100096.

The solid oxide fuel cell-gas turbine (SOFC-GT) hybrid system is among the most efficient power generation technologies. However, the development of SOFCs has focused on lower operating temperatures, which is much lower than the turbine inlet temperature (TIT) of the advanced hundred-MW-class gas turbines (GTs) ($>$ 1400°C), hindering their integration. Therefore, current large-scale GTs still primarily enhance power generation efficiency by increasing TIT, which approach has suffered from prominent marginal effects, leading to the bottleneck in efficiency enhancement. To address this, we propose a super-high-temperature SOFC operating at above 1200°C, which can be integrated with a commercial hundred-MW-class gas turbine to break the efficiency bottleneck. In our laboratory, a single tubular SOFC achieved a peak output power of 4.67 W at 1200°C, which is 5.5 times higher than that at 700°C. We simulated a hundred-MW-class hybrid system to demonstrate the necessity of the elevation of SOFCs temperature, analyzing it thermodynamically based on a T-s indicator diagram. When the SOFC operating temperature increases from 800°C to 1200°C, the temperature mismatch degree between the SOFC and the F-class gas turbine decreases significantly from 68.16% to 0%. This improvement is accompanied by an increase in fuel cell combustor (FCC) exergy efficiency from 76.52% to 85.93%, and an increase in system efficiency from 58.60% to 74.12%. Further elevating the SOFC operating temperature to approximately 1300°C could potentially yield a system efficiency of 80.31%. Considering these substantial thermodynamic advantages, we propose a new development route for SOFCs towards a super-high operating temperature of over 1200°C.

INTRODUCTION

In the last few decades, owing to vigorous industrialization, large amounts of CO_2 and other pollutants have been emitted into the environment, leading to severe undesirable effects such as global warming. Highly efficient power generation technologies are constantly being pursued and developed to achieve sustainable development.

Solid oxide fuel cell-gas turbine (SOFC-GT) hybrid system is one of the most efficient power generation devices among various technologies, which can achieve efficiencies higher than 70%.[1,2] The ultrahigh efficiency of the SOFC-GT hybrid system mainly results from its cascade energy utilization: the chemical energy in the fuel is directly converted into electricity by the SOFC, and the high-quality heat in the exhaust gas is further converted into electricity by the downstream turbine. The configuration of the SOFC-GT hybrid system can be divided into two categories, which are indirect and direct.[3] In the indirect configuration, the SOFCs operate in an atmospheric environment and serve as a subsystem separated by a heat exchanger that is completely independent of the turbine, allowing safe and robust operation. In the direct configuration, the SOFC stack and downstream burner serve as the combustor of the turbine, which is called fuel cell combustor (FCC) in this study, and the SOFC stack is strongly coupled with the downstream turbine, which requires a good temperature match. Because the SOFC stack operates under pressurized conditions, higher system efficiency can be achieved, and the direct configuration is preferred and mostly selected.[1] Several direct-type, hundred-kilowatt-class prototypes were designed and constructed. Siemens Westinghouse manufactured a 220 kW SOFC-GT hybrid system fueled by natural gas and achieved an overall electrical efficiency of 52.44%.[4] Mitsubishi Heavy Industries fabricated a 250 kW-class SOFC-MGT hybrid system with an efficiency of 55%.[5] Moreover, significant efforts have been devoted to system design and parameter optimization based on simulation.[6-10] Researchers have combined SOFC-GT systems with other bottom cycles, such as the organic Rankine cycle (ORC)[11,12] and steam turbine cycle[13] to achieve further waste heat recovery, so that a higher efficiency can be achieved. In recent years, machine learning has been utilized to achieve the multi-objective optimization and assist the performance analysis, which is an effective strategy for the system research.[14,15]

However, as the core components of the SOFC-GT hybrid system, the development trends of the operating temperatures of the SOFCs and GTs are in opposite directions, as shown in Figure 1, which leads to a significant temperature mismatch and hinders their coupling. The main development trend in SOFCs is to lower the operating temperature, which is expected to reduce their costs and degradation rates.[16,17] By using highly active materials and designing nano-scale structure, SOFCs can operate at temperatures even lower than 600°C in laboratory.[18,19] In contrast, a higher turbine inlet temperature (TIT) is constantly pursued in the R&D of GTs, which is thermodynamically beneficial for improving the Brayton cycle efficiency. For example, the TIT of gas turbine has been elevated from 1000°C for micro gas turbine to advanced J-class gas turbine for 1600°C, which can achieve a combined cycle efficiency of 62%, and the output power can reach 200 MW.[20] However, the TIT of the advanced GTs is much higher than SOFCs, which hinders their coupling in SOFC-GT hybrid system, and most research in this field is still conducted based on conventional GTs with TIT lower than 1200°C,[8,21-23] which makes it difficult to make substantial breakthroughs. The low TIT of the downstream turbine significantly hindered the thermal efficiency improvement of the Brayton cycle, limiting the efficiency improvement of the hybrid system. Adding extra fuel to the downstream burner can effectively increase the TIT, but it can lead to a significant exergy loss in FCC, which will be discussed in detail in this study. In addition, due to the temperature mismatch with conventional SOFC, the hundred-MW-class gas turbine still primarily enhance power generation efficiency by increasing the TIT, which approach has suffered from prominent marginal effects,[24] leading to the bottleneck in the efficiency enhancement.

Based on the analysis above, elevating the SOFC operating temperature can achieve the temperature match with advanced gas turbine, which facilitates their integration, thereby overcoming the current efficiency improvement bottleneck of large-scale GTs. In this paper, a super-high-temperature SOFC (SHT-SOFC) operating at 1200°C is proposed and preliminary verified by experiment. Then, the necessity of elevating the SOFC operating temperature in a hundred-MW class SOFC-GT hybrid system is demonstrated by a system-level simulation, which is analyzed from a thermodynamic perspective based on the temperature entropy (T-s) indicator diagram. Finally, considering the huge thermodynamic advantages, we propose a new development route for SOFCs towards a super-high operating temperature of over 1200°C.

THEORY

The effect of elevating the SOFC operating temperature on the improvement of system efficiency can be visually represented based on a thermodynamic spectrum of T-s indicator diagram, which is a powerful tool for analyzing the energy conversion process in conventional thermodynamic cycles such as the Brayton and Rankine cycles. The amount of heat absorbed or released during a thermodynamic process can be visualized by the area

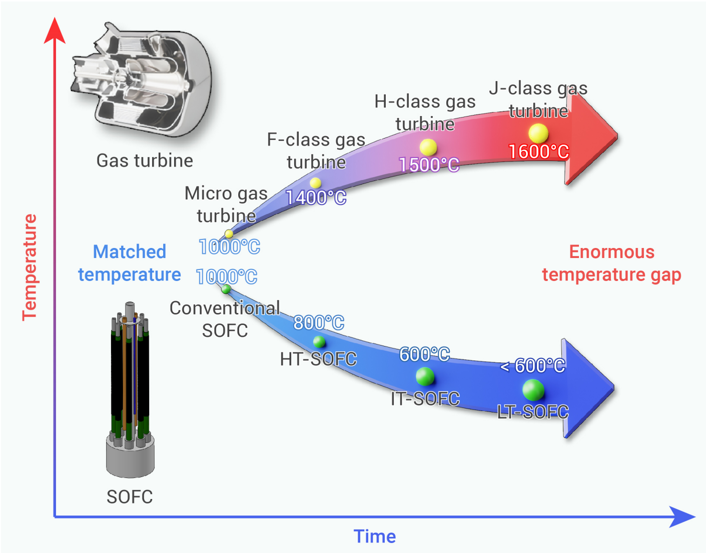

Figure 1. Comparison of the development trends between GTs and SOFCs.[20,25] (Adapted with permission from Li et al.,[25] Copyright 2023 Elsevier under CC BY-NC-ND 4.0)

enclosed by the corresponding line and abscissa in the T-s diagram. Moreover, for an ideal Brayton cycle without a recuperator, the mechanical energy output of the system can be represented by the difference between the areas of the endothermic and exothermic processes based on the energy conservation law. For the SOFC-GT hybrid system, the thermodynamic cycle involves the conversion of chemical energy into electricity, which cannot be directly represented in the T-s indicator diagram. Although some researchers have analyzed the thermodynamic cycle of SOFC-GT hybrid systems based on T-s indicator diagrams, their main role in the analysis was to demonstrate the thermodynamic properties of specific nodes, while the most powerful function that expresses energy in terms of area was neglected.[26,27]

Although the electricity generated in the SOFC-GT hybrid system cannot be directly represented in the T-s indicator diagram, it can be indirectly expressed by the area difference corresponding to the two thermodynamic processes, based on the energy conservation law. Figure 2A presents a simplified FCC diagram of the SOFC-GT hybrid system. Before entering the cathode chamber of the SOFC stack, the air is pressurized by a compressor and heated by a recuperator to T_1. The fuel enters the anode chamber and electrochemically reacts with oxygen in cathode air to generate electricity. The temperatures of the anode and cathode exhaust are equal to the SOFC operating temperature, T_2. Finally, the exhausts enter the downstream burner, where the unreacted fuel is completely burned and the exhaust gas temperature reaches a higher temperature of T_3. Figure 2B shows a T-s indicator diagram corresponding to the thermodynamic processes in the FCC. Because the mass flow rate of air in the FCC is much higher than that of fuel, the thermodynamic properties of the working fluid can be approximated to those of air, and the T-s curve in Figure 2B is the temperature of air as a function of the specific entropy at the operating pressure of the SOFC stack, which can be obtained using REFPROP software. The thermodynamic processes in the SOFC stack (b→c) and downstream burner (c→d) are shown in Figure 2B. The area *abch* (S_{abch}) represents the heat generated in the SOFC stack. S_{hcdg} represents the heat generated in the downstream burner, which is equal to the chemical energy of the unreacted fuel in the anode exhaust. Assuming that air and fuel with the same thermodynamic properties and mass flow rate are directly combusted in a burner, the temperature of the exhaust will reach T_c in Figure 2B, which is higher than T_3, because all the chemical energy in the fuel is converted into heat. Therefore, the chemical energy of the fuel can be expressed in Figure 2B as S_{abef}. Based on the energy conservation law, electricity is equal to the difference between the chemical energy in the fuel S_{abef} and the thermal energy S_{abdg}. Therefore, the electrical power generated by the SOFC stack can be expressed as S_{gdef} in the T-s diagram.

The area shown in the T-s indicator diagram can be correlated with the

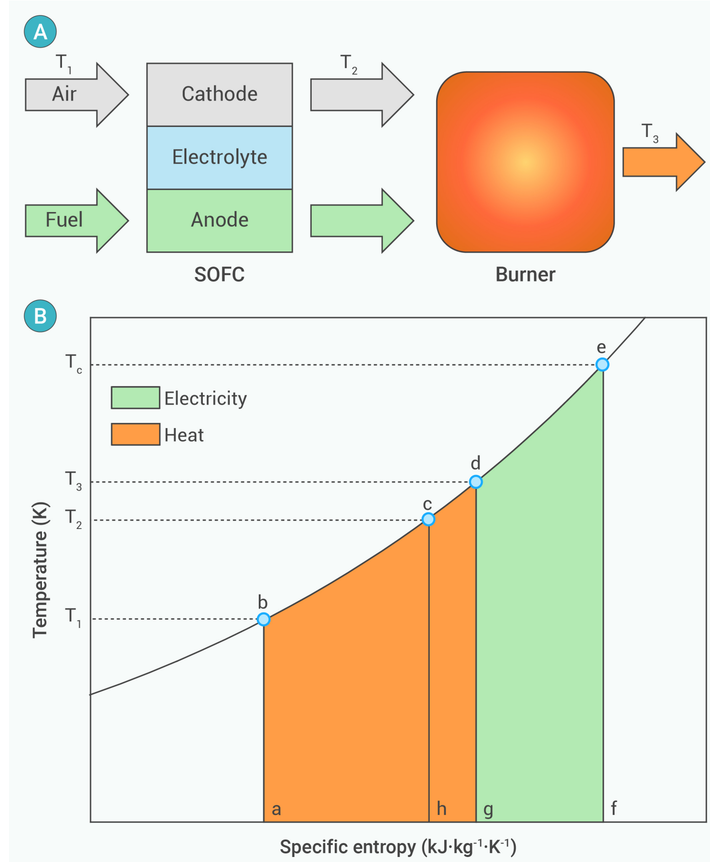

Figure 2. Thermodynamic analysis of FCC (A) Simplified diagram of FCC in SOFC-GT hybrid system. (B) Corresponding T-s indicator diagram.

operating parameters of the SOFC stack. For the SOFC-GT system, the output voltage of a single-cell V and the fuel utilization factor u_{fuel} of the entire stack are usually adjusted to ensure that the SOFC stack operates in a reasonable state. The electrical efficiency of the SOFC stack can be expressed as

$$\eta_{SOFC}=\frac{P_{SOFC}}{\dot{n}h_{fuel}}=u_{fuel}\frac{k_sk_pIV}{\dot{n}_{react}h_{fuel}}=u_{fuel}\frac{NFV}{h_{fuel}} \quad (1)$$

where P_{stack} is the total output power of the SOFC stack, $\dot{n}$ is the molar flow rate of the fuel, $\dot{n}_{react}$ is the molar flow rate of the fuel reacted in the SOFC stack, h_{fuel} is the low heating value of the fuel, u_{fuel} is the fuel utilization factor, k_s and k_p are the number of cells in series and parallel, I and V are the current and voltage of a single cell, N is the number of electrons transferred in the reaction, and F is Faraday's constant, 96485 C/mol.

The area representing the total chemical energy in fuel can be expressed as:

$$S_{abef}=\dot{n}h_{fuel} \quad (2)$$

The area representing the output electricity of the SOFC stack can be expressed as:

$$S_{gdef}=P_{SOFC}=\eta_{SOFC}S_{abef}=u_{fuel}\frac{NFV}{h_{fuel}}S_{abef}=\dot{n}u_{fuel}NFV \quad (3)$$

In the burner, the generated heat is equal to the chemical energy in the unreacted fuel in the anode exhaust and can be expressed as:

$$S_{hcdg}=(1-u_{fuel})S_{abef}=(1-u_{fuel})\dot{n}h_{fuel} \quad (4)$$

Based on the energy conservation law, the area representing the heat released in the SOFC stack can be expressed as follows:

$$S_{abch}=S_{abef}-S_{gdef}-S_{hcdg}=\dot{n}u_{fuel}(h_{fuel}-NFV) \quad (5)$$

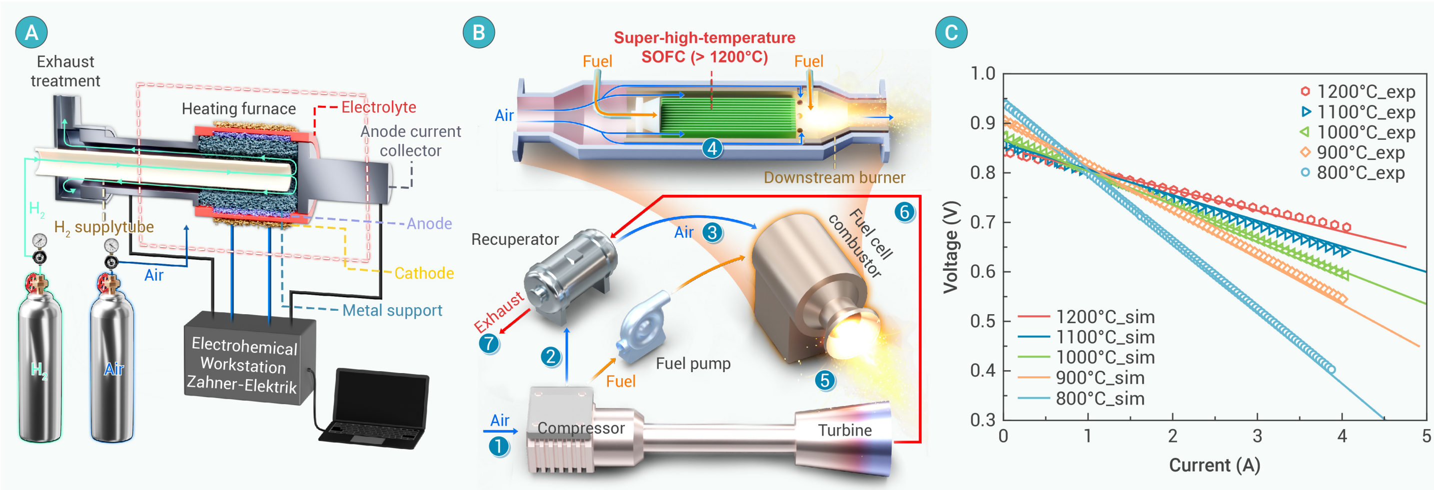

Figure 3. Experimental and system modeling (A) Experimental system of the tubular metal-supported SOFC. (B) Schematic of the SOFC-GT hybrid system. (C) Comparison between model results and experimental data.

MATERIALS AND METHODS

Experimental

Cell fabrication. A single tubular SOFC was prepared in our laboratory by thermal spraying to demonstrate the feasibility of SHT-SOFC operating at 1200°C. The current collecting at 1200°C was achieved by welding technology based on the metal-supported configuration. A single tubular SOFC was supported by a porous 430 stainless steel substrate (Nanjing Gaoqian Functional Material Technology Co., Ltd., China) with a thickness of 1 mm, length of 100 mm, and outer diameter of 20 mm. The metal-supported configuration is selected due to its high mechanical strength and robustness, which enables the resistance of the high thermal stress at super high operating temperature. A steel plug was welded to one end of the tubular metal support using laser welding to form a blind tube. The functional layers of the anode, electrolyte, and cathode were prepared by thermal spraying on the surface of the metal substrate; the spraying parameters are listed in Table S1. Atmospheric plasma spraying (APS) was used to deposit the anode layer of 40 μm with NiO/YSZ agglomerated powders at a plasma arc power of 30 kW. The electrolyte layer was also deposited by APS at a plasma arc power of 44 kW. Due to the relatively high porosity of the YSZ electrolyte prepared by APS, the thickness of YSZ electrolyte is prepared as 600 μm to ensure the gas tightness. Moreover, a high thickness of YSZ electrolyte can significantly improve the robustness and mechanical strength, which avoids the crack at super high temperature due to thermal stress. Finally, the LSCF cathode was deposited by high velocity oxygen fuel (HVOF) with a thickness of 20 μm. The length of the cathode deposition area was 9 cm, and the active area of a single tubular metal-supported SOFC (MS-SOFC) was 56.5 cm^2.

Experimental setup. A schematic of the tubular MS-SOFC experimental system is shown in Figure 3A. The tubular SOFC was fixed in a heating furnace to achieve high-temperature operating conditions. The electrochemical performance of the SOFC was measured using a Zahner electrochemical workstation (IM6ex, Zahner-Elektrik GmbH, Germany) with 4-wire setup. Platinum wires (diameter: 0.3 mm) were used for the current collection at the cathode. To shorten the current transmission distance, platinum wires were wrapped on the cathode surface at 1 cm intervals. Two main collection lines were connected to an electrochemical workstation. Current collection at the anode was achieved using a steel tube and steel column, which were welded at the open and blind sides of the tubular SOFC, respectively. The ends of the steel current-collecting tube and column were extended to the outside of the furnace and connected to an electrochemical station using silver wires. In this design, the resistances of the steel current-collecting tube and column were eliminated based on a 4-wire setup so that the electrochemical performance of the SOFC could be measured accurately. An aluminum tube was inserted into the tubular SOFC to supply hydrogen. Air was supplied to the furnace during the experiment.

Experimental procedure. After setting up the experimental system, the tubular MS-SOFC was heated at a rate of 3°C/min. During the heating process, hydrogen was supplied to the tubular SOFC at a flow rate of 100 standard cubic centimeters per minute (SCCM), which maintained a reductive atmosphere to reduce NiO to Ni. Air was supplied to the furnace at a flow rate of 200 SCCM. When the temperature reached a target value, the open-circuit voltage (OCV) was measured until a stable value was reached. The electrochemical performance of the tubular MS-SOFC was measured using an electrochemical workstation. Current-voltage (I-V) curves were obtained by scanning the OCV voltage at a speed of 5 mV/s. The EIS (electrical impedance spectra) tests were performed in the OCV state with an AC amplitude of 10 mV. The test frequencies ranged from 30 kHz to 0.1 Hz.

Modeling

System description. A schematic of the SOFC-GT hybrid system simulated in this study is shown in Figure 3B, which was simulated based on the gRROMs ModelBuilder, as illustrated in Figure S1. The basic configuration of the hybrid system is consistent with that of a conventional gas turbine cycle with recuperation,[26,28] whereas the main difference is the substitution of a conventional combustor into an FCC comprising an SOFC stack and a downstream burner. The operating temperature of the SOFC stack was regulated by adjusting the air mass flow rate. If the temperature of the FCC exhaust gas is lower than the required TIT, additional fuel is added directly to the downstream burner to compensate for the temperature gap.

System thermodynamic-economic model and validation. The SOFC stack was simulated based on a multilevel model, including the positive-electrolyte-negative (PEN), cell, and stack levels, which has described in detail in the Supplemental Information. The SOFC model was validated by comparing the simulation and experimental results. The geometric and electrochemical parameters are summarized in Table S2. The SOFC geometric parameters in the simulation are consistent with those of the tubular SOFC prepared in Section 2.1. The experimental polarization curves between 800°C and 1200°C were measured in a furnace with H_2 flow rate of 100 SCCM. Based on Figure 3C, the polarization curves produced by the SOFC model show high agreement with the experimental results, which validates the reliability of the SOFC model.

The balance of plant (BOP) components of the SOFC-GT hybrid system comprise a heat exchanger, a compressor, two turbines, a mixer, and several pipes. These models are obtained from related references.[29-31] In the previous study of our group, a SOFC-GT hybrid simulation system was constructed based on these BOP models, which has been validated in system level by comparison with the experimental data of the Siemens–Westinghouse 220 kW SOFC–GT hybrid generation system,[29] demonstrating the reliability the BOP models used in this study. Therefore, the calculation results are credible with an acceptable range of error.

The economic model of the hybrid system is described in Supplemental Information, which mainly includes the calculation of the levelized cost of electricity (LCOE) and payback period. The calculation of the component investment costs is listed in Table S3.

System evaluation parameters. The entire system is evaluated using the system efficiency η_{sy}, which is defined as:

$$\eta_{sy} = \frac{P_{SOFC} + P_{turbine}}{\dot{n}h_{fuel}} \quad (6)$$

where $P_{turbine}$ is the net output power of the turbine.

The evaluation parameter of the FCC is the exergy efficiency η_{ex} defined as:

$$\eta_{ex} = 1 - \frac{Ex_{loss}}{Ex_{in}} = 1 - \frac{Ex_{air} + Ex_{fuel} - Ex_{exhaust} - P_{SOFC}}{Ex_{fuel}} \quad (7)$$

where Ex_{loss} represents the total exergy loss in the FCC, Ex_{in} represents the input exergy of the fuel, Ex_{air} represents the exergy of the inlet air, and $Ex_{exhaust}$ represents the exergy of the FCC exhaust.[32]

In the SOFC-GT hybrid system, SOFCs serve as the combustor of the turbine, which requires matched operating temperatures. However, the inlet temperature of a hundred-MW-class gas turbine is generally higher than 1400°C,[20] whereas the operating temperature of conventional SOFCs is lower than 1000°C, which leads to a high degree of temperature mismatch. To compensate for this temperature gap, a certain amount of fuel must be added directly to the downstream burner to increase the temperature of the FCC exhaust. Because a higher temperature gap requires more fuel to be added to the lean combustor, the degree of temperature mismatch can be described by the proportion of the added fuel χ_{add}, which is defined as:

$$\chi_{add} = \frac{\dot{n}_{fuel,add}}{\dot{n}_{fuel,SOFC} + \dot{n}_{fuel,add}} \quad (8)$$

where $\dot{n}_{fuel,SOFC}$ is the molar flow rate of the fuel entering the SOFC stack and $\dot{n}_{fuel,add}$ is the fuel molar flow rate directly added to the downstream burner.

RESULTS AND DISCUSSION

Development of SHT-SOFC

The concept of SHT-SOFC operating at 1200°C was firstly validated based on a tubular SOFC fabricated in our laboratory by plasma spraying. The electrochemical performance of the tubular SOFC under operating temperatures of 700°C, 800°C, 900°C, 1000°C, 1100°C, and 1200°C was measured, as shown in Figure 4. The maximum measured current of the electrochemical workstation used in this experiment is 4 A, in which case the tubular SOFC has not reached the peak power output in the operating temperature higher than 900°C. Because the cell output voltage decreased nearly linearly with an increase in current density, the portion of the data where the current was higher than 4 A was extrapolated using a linear extension,[33] which allowed for the calculation of the peak power output.

As shown in Figure 4A, the tubular SOFC showed an OCV of 0.977 V and 0.843 V at 700°C and 1200°C, respectively, which is lower than the theoretical OCV. The reduced OCV indicates that the YSZ electrolyte fabricated by APS was not fully dense,[34] which can be improved using very low-pressure plasma spraying (VLPPS) in future studies.[35] As can be seen from the I-V curves in Figure 4A, when the SOFC operating at a conventional temperature of 700°C, the peak power of the tubular SOFC was 0.85 W. In contrast, when the operating temperature was elevated to 1200°C, the peak power significantly increased for 5.5 times and reached 4.67 W, which achieved almost an order of magnitude improvement.

To reveal the reasons for the performance improvement, the impedance spectra of the tubular SOFC at different operating temperatures were measured to separate the ohmic and polarization resistances, as shown in Figure 4B. In conventional operating temperature of 700°C, the electrochemical performance of SOFC is mainly limited by the ohmic resistance, which is 239 mΩ, accounting for 85% of the total resistance. The high ohmic resistance mainly results from the medium ionic conductivity of the YSZ electrolyte. Moreover, although the polarization resistance of 41 mΩ only accounts for 15% of the total resistance, the EIS curve mainly comprises a large semicircle at high frequency zone (>10 Hz), which corresponds to the processes of oxygen ionic transport, charge transfer reaction within the anode as well as oxygen surface exchange reaction within the cathode,[36] indicating that reaction kinetics of electrode at 700°C is limited. When the SOFC operating temperature was elevated to 1200°C, the ohmic resistance was significantly reduced to 26 mΩ, which decreased for almost an order of magnitude compared with 700°C. The reduced ohmic resistance results mainly from the enhanced oxygen ion conductivity of the YSZ electrolyte. Moreover, the activation impedance semicircle gradually decreases with the temperature increasing and finally disappears at 1200°C, indicating the significantly improvement of electrode reaction kinetics, which led to a reduced polarization of 16 mΩ. In summary, it is precisely because of the reaction kinetics advantage at an elevated temperature of 1200°C that the SOFC achieves an order-of-magnitude increase in output power.

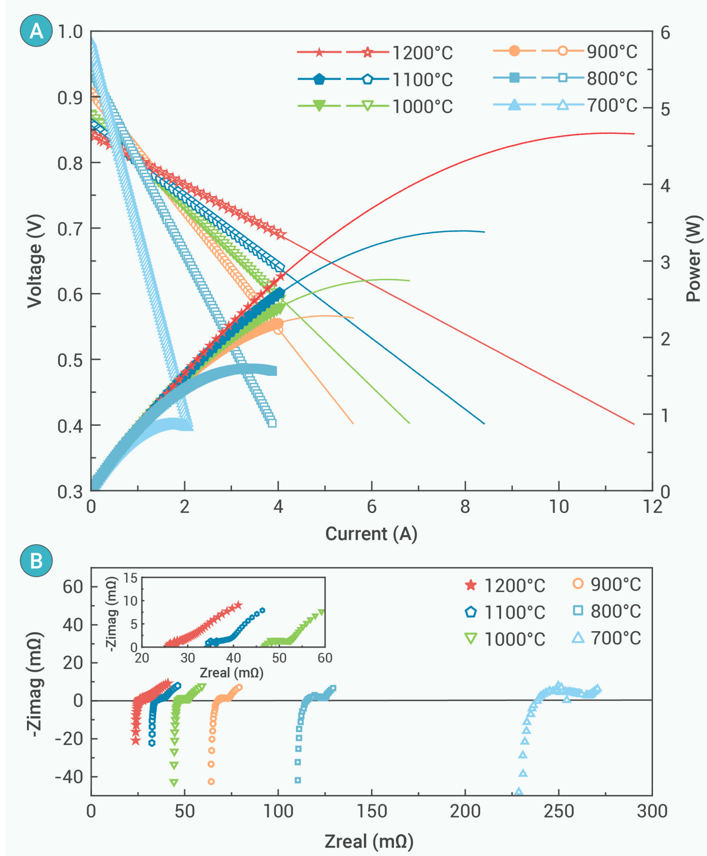

Figure 4. Electrochemical performance of the thermal-sprayed tubular SOFC under various operating temperatures (A) Polarization curves. (B) EIS curves.

Thermodynamic analysis of the hundred-MW-class SOFC-GT hybrid system

Base case results. To demonstrate the necessity of elevating the SOFC operating temperature for a hundred-MW-class SOFC-GT hybrid system, we simulate the hybrid system with SOFC operating at temperatures from 800°C to 1200°C, and the operation parameters are listed in Table S4. The total output power was 200 MW. The pressure ratio was set as 18, which is consistent with a commercial hundred-MW-class gas turbine.[20] The voltage of a single cell is 0.7 V, and the fuel utilization factor is 0.85. Hydrogen was used as fuel for the hybrid system. Based on the simulation results, when the SOFC stack operates at an elevated temperature of 1200°C, the TIT can reach 1424°C (1697 K) without added fuel into downstream burner, close to the TIT of F-class gas turbine for 1400°C,[20] which makes it possible to coupling the SHT-SOFC with commercial hundred-MW-class gas turbine. For the simulation of the hybrid system with SOFC operating at 800°C, 900°C, 1000°C, 1100°C, as well as the gas turbine system, extra fuel is added into the downstream burner to enable TIT to also reach 1697 K. The simulation results are listed in Table S5.When the SOFC operates at an elevated temperature of 1200°C, 85% of the supplied fuel is efficiently utilized by the SOFC stack, which generates an electrical power of 127.91 MW. Since the temperature of SHT-SOFC matches well with downstream turbine, no extra fuel is added to

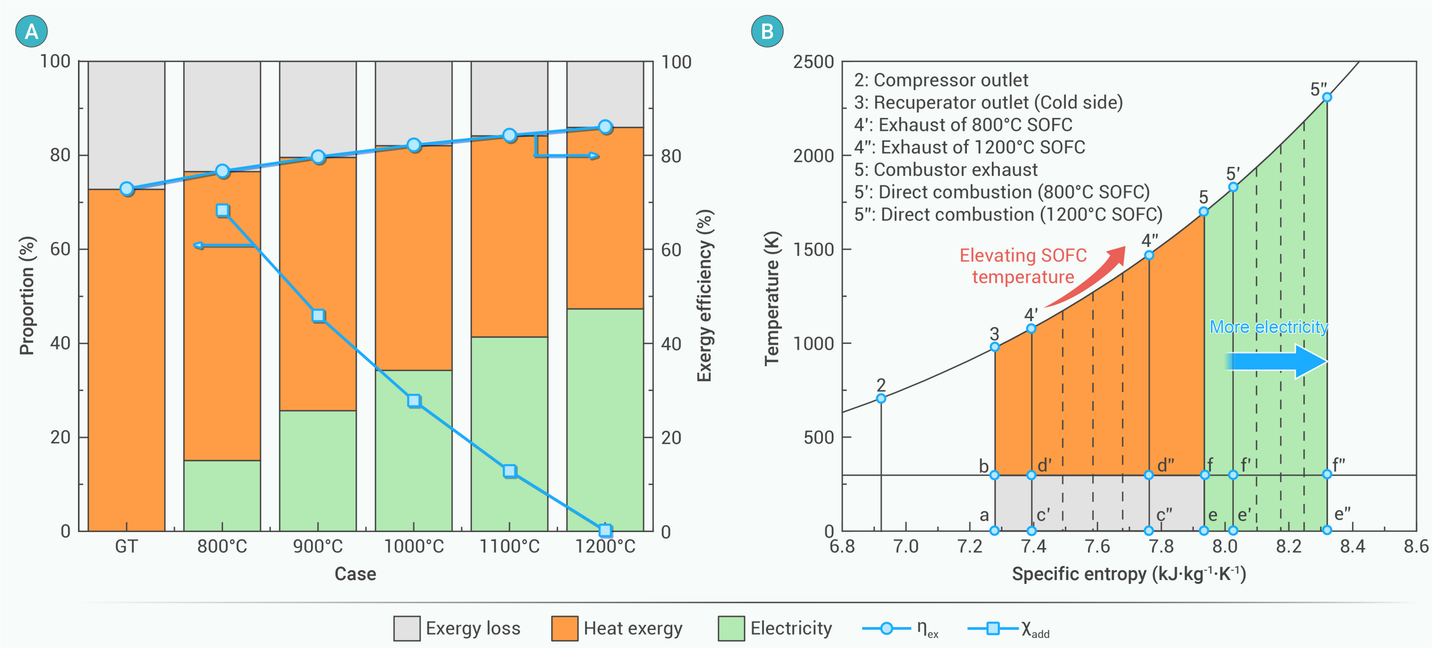

Figure 5. Simulation results and thermodynamic analysis of FCC (A) Exergy loss, heat exergy, electricity, η_{ex}, and χ_{add} in the gas turbine system and SOFC-GT hybrid system with the SOFC operating at different temperatures. (B) The corresponding T-s indicator diagram in a conventional combustor or FCC.

the burner. The exergy efficiency of the FCC reached 85.93% and the system efficiency reached 74.12%. In contrast, when the SOFC stack operates at a conventional temperature of 800°C, over 70% of the fuel (including unreacted fuel in the SOFC stack) is directly combusted in the downstream burner to compensate for the large temperature gap between the SOFC and the downstream turbine, leading to a high temperature mismatch degree of 68.16%. This process inhibits the high-efficient energy conversion advantage of the SOFC, resulting in a low system efficiency of 58.60%. Consequently, the hybrid system operates close to a gas turbine system. Based on the simulation results, elevating the SOFC temperature to lower the degree of temperature mismatch between the SOFC and the gas turbine is necessary for a hundred-MW-class hybrid system. This necessity is analyzed from a thermodynamic perspective using a T-s indicator diagram.

Thermodynamic analysis of FCC. In the FCC, the chemical exergy in the fuel is converted into heat exergy, electricity, and exergy loss; their proportions are shown in Figure 5A based on the simulation results. Compared to a conventional combustor in a GT system, an FCC can achieve a higher exergy efficiency owing to the high-efficiency energy-conversion process in the SOFC. As the SOFC temperature increases from 800°C to 1200°C, the temperature gap between the SOFC and the TIT (1697 K, 1424°C) narrows, resulting in a reduction of the temperature mismatch. Consequently, χ_{add} decreases from 68.16% to 0%, and more fuel is electrochemically converted in the SOFC to generate electricity rather than being combusted in the downstream combustor, which leads to a gradual increase in the proportion of electrical energy generated by the SOFC within the FCC, while the proportion of heat exergy production gradually decreases. Nevertheless, the total exergy efficiency of the FCC improves from 76.52% to 85.93%, which that can be further illustrated based on a T-S diagram.

The T-s indicator diagram of the FCC in the SOFC-GT hybrid system, as well as that of the conventional combustor in a gas turbine system, is shown in Figure 5B. Based on the theory constructed in Section 2, the heat exergy of the combustor can be represented by the orange area S_{b35f}, while the electrical energy in the FCC is denoted by the green area $S_{e55''e''}$. Based on the T-s diagram, the conversion of fuel chemical energy into heat inevitably accompanies the generation of anergy, corresponding to the grey area S_{abfe}, which is the exergy loss in FCC. In contrast, the conversion of chemical energy into electricity can avoid this loss. Therefore, when the SOFC operates at a higher temperature, a larger proportion of the chemical energy in the fuel is converted into electricity rather than heat, leading to an increase in the overall exergy efficiency of the system.

Specifically, the point numbers in T-s diagram correspond to the nodes in Figure 3B. Point 3 refers to the air pressurized by the compressor and heated by the turbine exhaust gas in the recuperator. Since all the cases keep the same compression ratio of 18 and TIT of 1697 K (1424°C), the temperature of the turbine exhausts exhibits the same temperature of 1009 K (736°C), which heats the air before entering the FCC to a constant T_3 of 976 K (703°C) in all cases. Points 4′ and 4″ refer to the exhaust of the SOFC stack, whose temperature is equal to the SOFC operating temperature. For the simulation cases of the SOFC-GT hybrid system, the operating temperature gradually increases from 1073 K (800°C, point 4′) to 1473 K (1200°C, point 4″). Point 5 refers to the exhaust of the conventional combustor or FCC, which was set to a consistent temperature of 1697 K (1424°C). As illustrated in Section 2, to represent the electrical power in the T-s indicator diagram, the direct combustion temperature corresponding to the FCC is required, which is the exhaust gas temperature resulting from the combustion of fuel and air with the same thermodynamic properties and mass flow rate directly entering the combustor without passing through the SOFC, corresponding to the condition where the chemical energy in the fuel is entirely converted into thermal energy. When the SOFC operating temperature increases from 800°C to 1200°C in FCC, the direct combustion temperature increases from 1822 K (1549°C, point 5′) to 2309 K (2036°C, point 5″), so that the area corresponding to electrical power P_{SOFC} expands from $S_{e55'e'}$ to $S_{e55''e''}$. In the FCC, all exergy in the fuel is converted into heat exergy Q_{ex}, SOFC electrical power P_{SOFC}, and exergy loss Ex_{loss}. Therefore, the exergy efficiency of the FCC can be expressed as a combination of the following areas:

$$\eta_{ex}=1-\frac{Ex_{loss}}{Ex_{Fuel}}=1-\frac{Ex_{loss}}{Q_{ex}+Ex_{loss}+P_{SOFC}}=1-\frac{S_{abfe}}{S_{b35f}+S_{abfe}+S_{electricity,SOFC}} \quad (9)$$

The S_{b35f} corresponding to the heat exergy and S_{abfe} corresponding to the exergy loss remain unchanged because all cases maintain the same inlet and outlet temperatures of the FCC. S_{a35e} represents the summary of the heat exergy and exergy loss in the FCC, which is also kept constant in all cases. For the area $S_{electricity,SOFC}$ corresponding to the SOFC electrical power, it expands from $S_{e55'e'}$ to $S_{e55''e''}$ with the SOFC operating temperature increasing from 800°C to 1200°C. Therefore, a higher SOFC operating temperature leads to a higher exergy efficiency based on Equation 9.

As shown in Figure 5B, the operating temperature of the SOFC significantly affects its electrical power. According to Equations 3 & 5, the ratio of the electrical power to the heat generated in the SOFC k can be expressed as:

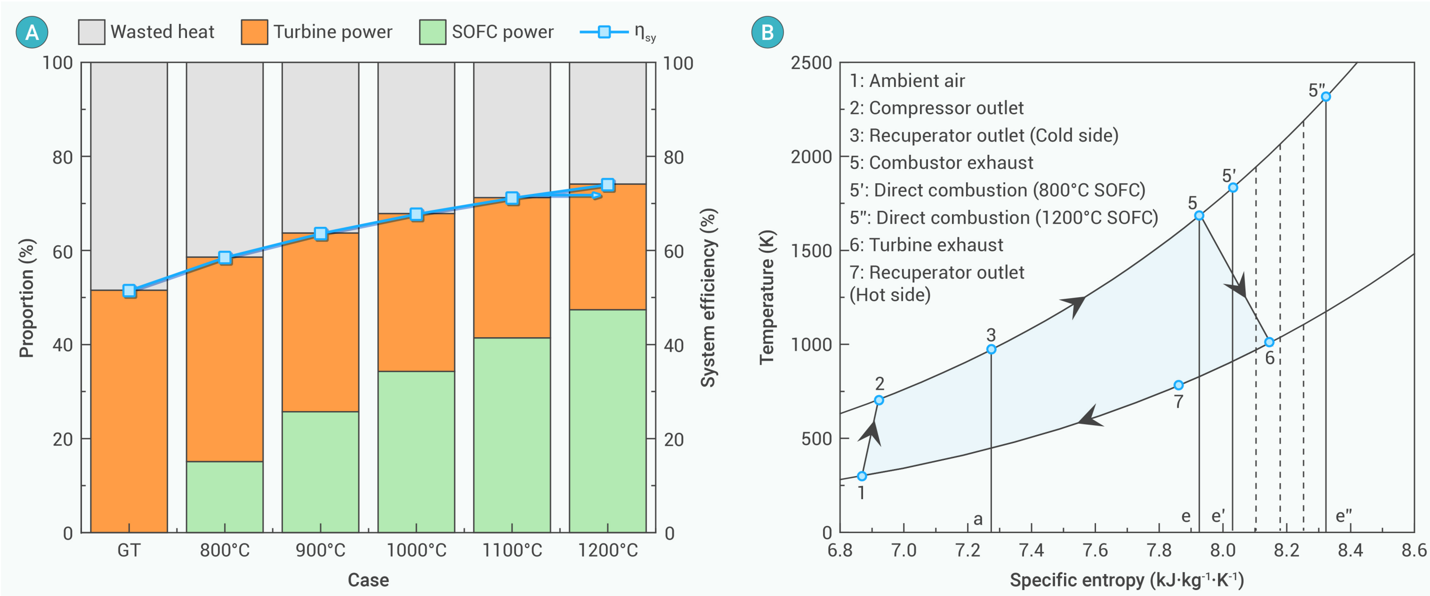

Figure 6. Simulation results and thermodynamic analysis of SOFC-GT hybrid system (A) Proportions of SOFC electrical power, turbine power, waste heat, and system efficiency in different cases. (B) The corresponding T-s indicator diagram of the thermodynamic cycle.

$$k = \frac{S_{electricity,SOFC}}{S_{heat,SOFC}} = \frac{NFV}{h_{fuel} - NFV} \quad (10)$$

In all simulation cases, the single cell voltage V is set as 0.7 V, which leads to a constant ratio k. When the operating temperature increases from 800°C to 1200°C, the area corresponding to the heat generated in SOFC $S_{heat,SOFC}$ expands from $S_{a34'c'}$ to $S_{a34''c''}$. Therefore, the area of SOFC electric power $S_{electricity,SOFC}$ also proportionally increases from $S_{e55''e''}$ to $S_{e55''e''}$.

Additionally, compared to traditional combustors, the FCC enables "electrochemical cooling" of the exhaust gas, whereby the energy in the fuel is output in the form of electrical power, thereby reducing the temperature of the exhaust gas. For example, in the case of SOFC operating at 1200°C, since 47.40% energy in fuel is converted into electricity ($S_{e55''e''}$) by SOFC, the temperature of the exhaust gas is reduced from 2309 K (2036°C, point 5″) to 1697 K (1424°C, point 5). In contrast, for the conventional combustor in gas turbine system, the main method to lower the exhaust temperature is increasing the excess air ratio, which makes the chemical energy in fuel be "diluted" and reduces the quality of energy, leading to more exergy loss. The area $S_{eff'e''}$ corresponds to the exergy loss in the direct combustion process that can be converted into electricity by the SOFC stack in the FCC; thus, the exergy efficiency increases from 81.55% to 85.93%. Therefore, FCC can achieve the reduction of the exhaust temperature by "electrochemical cooling" while increase the exergy efficiency.

Thermodynamic analysis of the whole system. For the entire SOFC-GT hybrid system, the input chemical energy in the fuel is converted into SOFC electrical power, turbine power, and waste heat. Their proportions as well as the system efficiency η_{sy} in different cases are shown in Figure 6A. When the SOFC operates at 800°C, the system efficiency is only 58.60%, which only achieves 7.06% efficiency improvement compared to conventional GT system. Under these conditions, owing to the high temperature gap between the SOFC (800°C) and the downstream turbine (1424°C), their temperature mismatch degree reached 68.16%, and over 70% of the fuel is directly combusted to generate heat, which can only be further converted into electricity by the turbine. However, due to the complex energy conversion processes, the efficiency of the turbine is significantly diminished, leading to a moderate system efficiency of 58.60%. In contrast, when the SOFC operating temperature gradually increases from 800°C to 1200°C, the temperature mismatch degree decreases to 0%, and more chemical energy in fuel is directly converted into electricity by SOFC, and the proportion of electricity generated by SOFC increases from 25.76% to 63.95%, leading to a system efficiency improvement from 58.60% to 74.12%.

The improvement in system efficiency with an increase in the SOFC operating temperature can also be illustrated from the perspective of thermodynamics based on the T-s indicator diagram in Figure 6B. The system efficiency can also be expressed as a combination of areas in the T-s indicator diagram as follows:

$$\eta_{sy} = \frac{P_{turbine} + P_{SOFC}}{Q_{Fuel}} = \frac{S_{TP} + S_{electricity,SOFC}}{S_{a35e} + S_{electricity,SOFC}} = 1 - \frac{S_{a35e} - S_{TP}}{S_{a35e} + S_{electricity,SOFC}} \quad (11)$$

Since all of the cases keep the same pressure ratio of 18 and TIT of 1424°C, per unit working fluid mass flow rate process approximately the same output power S_{TP} in turbine. S_{a35e} corresponds to the heat generated in FCC or conventional combustor, which also keeps a constant area. With the increase of SOFC operating temperature, the area of electrical power generated by the SOFC $S_{electricity,SOFC}$ gradually increases. Therefore, based on Equation 11, a higher system efficiency can be achieved.

Based on the simulation results, increasing the SOFC operating temperature will bring an obvious thermodynamic advantage to a hundred-MW-class hybrid system, which is validated by the increase in system efficiency. Moreover, the reaction kinetics of SOFCs can be effectively enhanced at elevated temperatures, which significantly decreases activation and ohmic loss. Therefore, the operating voltage can be increased appropriately from 0.7 V to 0.8 V, and the fuel utilization factor can also be increased from 0.85 to 0.95, so that a higher system efficiency can be achieved. Under the modified operating condition, when the SOFC operating temperature is further elevated to 1300°C, a super high system efficiency of 80.31% can be expected, which demonstrated the efficiency advantage of elevating SOFC operating temperature on SOFC-GT hybrid system. Moreover, SHT-SOFC can be coupled with the state-of-the-art gas turbines (TIT > 1400ºC) that have an ultra-high power density, thereby achieving an improvement in the overall power density of the hybrid power system. Simultaneously, the high energy efficiency advantage of SHT-SOFC can be utilized, allowing the entire system to achieve compatibility between high power density and high energy efficiency.

Figure 7 shows a comparison of the system efficiency and output power for the SOFC-GT hybrid system with different types of fuels, including hydrogen, biogas, ammonia, and methane. It can be seen that the current research is mainly based on simulations, which may be due to the high cost of the SOFC-GT hybrid system. Moreover, the system efficiency is generally lower than 70%, and the system output power ranges from the sub-MW class to the multi-MW class. In contrast, the highest system efficiency of 80.31% and largest output power of 200 MW were achieved in this study by integrating the SHT-SOFC with commercial F-class gas turbine, which breaks the bottlenecks of efficiency improvement and power amplification. Considering the huge thermodynamic advantages, elevating the SOFC operating temperature to above 1200°C is a promising development route.

Techno-economic analysis

Figure 8 presents the techno-economic analysis results of the 200 MW SOFC-GT hybrid power system, focusing on the variations in the system's LCOE and payback period with respect to the SOFC operating temperature and stack lifespan. Based on the results shown in Figure 8A, as the SOFC operating temperature increases, the system's LCOE gradually decreases, primarily due to enhanced power generation efficiency and reduced fuel costs. However, higher operating temperatures also lead to increased initial investment costs in SOFC stack, resulting in a longer payback period, as shown in Figure 8B.

On the other hand, as the SOFC stack lifespan extends, the system's LCOE gradually decreases, and the payback period is significantly shortened, leading to a notable improvement in techno-economic performance. This is attributed to the reduced frequency of SOFC stack replacements over the 20-year lifetime, thereby lowering investment costs. Notably, the effect of increasing the operating temperature on LCOE reduction becomes more pronounced with longer stack lifespans. For instance, when the stack lifespan is 10 kh, raising the temperature from 800°C to 1200°C only reduces the LCOE by 2.7%. However, when the lifespan is extended to 40 kh, the LCOE decreases from 0.1069 $/kWh to 0.0905 $/kWh, representing a reduction of 15.34%. Simultaneously, the negative impact of higher SOFC operating temperatures on the payback period diminishes as the stack lifespan increases. At a stack lifespan of 40 kh, the payback period for the 1200°C system is only 4.21 years, which falls within an acceptable range. Therefore, for the proposed SHT-SOFC-GT hybrid power system in this study, extending the SHT-SOFCs lifespan is crucial for improving its techno-economic performance.

PERSPECTIVE OF SHT-SOFCs

Currently, research on SOFCs is predominantly focused on the development of low-temperature operation. In contrast, this study innovatively proposes a different technological approach emphasizing high-temperature operation. It should be pointed that the proposition of this technological pathway is not intended to negate the prevailing trend of SOFC low-temperature development. Rather, it aims to expand the operational temperature range of SOFCs, thereby diversifying their application scenarios. This approach is expected to provide new technological pathways and theoretical foundations for advancing the large-scale commercialization of SOFCs.

In small-scale SOFC applications, such as compact cogeneration units and portable power systems, lower operating temperatures enhance compatibility with rapid start-stop cycles, mitigate carbon deposition, reduce metallic component corrosion, and extend SOFC lifespan. Additionally, low-temperature operation simplifies system packaging, lowering installation and maintenance costs, making it an inevitable trend for small-scale power systems. However, in the hundred-MW-class stationary power generation applications, such as large-scale gas power plant, achieving higher power generation efficiency is a more critical evaluation metric.

Currently, the gas turbine technology is still developing towards a higher TIT to further increase the thermal efficiency, while the marginal effects have already been very prominent, which has been validated by the slower increase in gas turbine efficiency in the last few decades.[24] Although SOFC-GT systems can achieve higher energy efficiency, the operating temperature of conventional SOFCs is incompatible with advanced hundred-MW-class gas turbines. To address this, this study proposes the concept of SHT-SOFCs, which can be coupled with advanced gas turbines to break the bottleneck in efficiency improvement. Furthermore, large-scale stationary power generation systems typically avoid frequent start-stop cycles, thereby reducing the demand for rapid thermal cycling. Techno-economic analysis reveals that the LCOE decreases significantly with increasing SOFC operating temperatures, and the economic advantages become more pronounced over long-term operation. Therefore, SHT-SOFCs is a potential candidate for the large-scale stationary power generation. However, for large-scale industrial applications, there are still several issues that need to be addressed with SHT-SOFCs.

(1) Durability: The SHT-SOFCs proposed in this study operate above

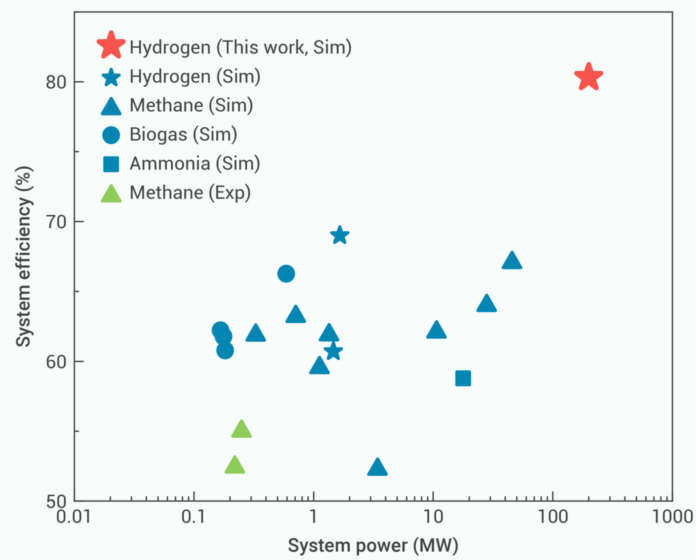

Figure 7. Comparison of the system efficiency and output power for SOFC-GT hybrid systems with different fuel types. [3-7,11-13,37-45]

1200°C, where extreme temperatures are inevitably accompanied by more severe durability issues that need to be addressed. The performance degradation of SHT-SOFCs primarily originate from two aspects: electrode microstructural deterioration and accelerated interfacial reactions. Conventional nickel-based or LSCF electrode materials are used in this study, and severe electrode sintering can be expected during long-term operating considering their relatively low melting points. This issue can be addressed by using high-melting-point materials like La-doped $SrTiO_3$ anodes and LSM cathodes for thermal stability. Moreover, the super-high operating temperature may induce electrode-electrolyte interfacial reactions during prolonged operation, which can be mitigated through barrier layer application. Benefiting from enhanced ionic conductivity of barrier materials at elevated temperatures, thicker layers become feasible in SHT-SOFCs, providing more effective suppression of interfacial degradation. Besides degradation from functional layers, prolonged super-high temperature operation can damage metal supports through sintering of porous structures, creep deformation, and hydrogen embrittlement, ultimately leading to structural failure and cell breakdown. To solve this issue, high-temperature alloys like HASTELLOY X [46,47] and Fe-10Al-4Cr-$_4Y_2O_3$,[48] used in gas turbines blades and combustor chamber, could serve as a promising candidate for metal supports and current collectors, offering excellent structure stability above 1200°C. Moreover, the high thermal conductivity of these alloys can effectively reduce temperature gradient,[49] which eases creep deformation due to thermal stress, while their low-stress static operation inherently limits hydrogen-driven crack growth.

(2) Power density: The elevated operating temperature of SHT-SOFC can significantly enhance the reaction kinetics of the cell, thereby improving the power density of the SOFC stack. The output power of SHT-SOFC at 1200°C (4.67 W) is more than twice that at 900°C (2.28 W), which can significantly reduce the volume of the SOFC stack and increase the system power density. However, the tubular configuration imposes structural constraint, which is not beneficial for the stack miniaturization. In future study, microtubular or planar SHT-SOFCs should be developed to make the entire stack more compact, thereby achieving higher volumetric power density.

(3) Multi-fuel compatibility: This study primarily focuses on the investigation of SHT-SOFCs under hydrogen fuel supply conditions. To further expand their applications, multi-fuel compatibility investigations towards hydrocarbon fuels such as methane are essential. Nevertheless, the elevated operating temperatures of SHT-SOFCs may accelerate hydrocarbon fuel cracking, potentially leading to more severe carbon deposition that limits practical applications. To address this challenge, SHT-SOFCs could substantially enhance the transport rate of oxygen ions to the fuel electrode at elevated temperature, potentially assisting in carbon deposition mitigation at the

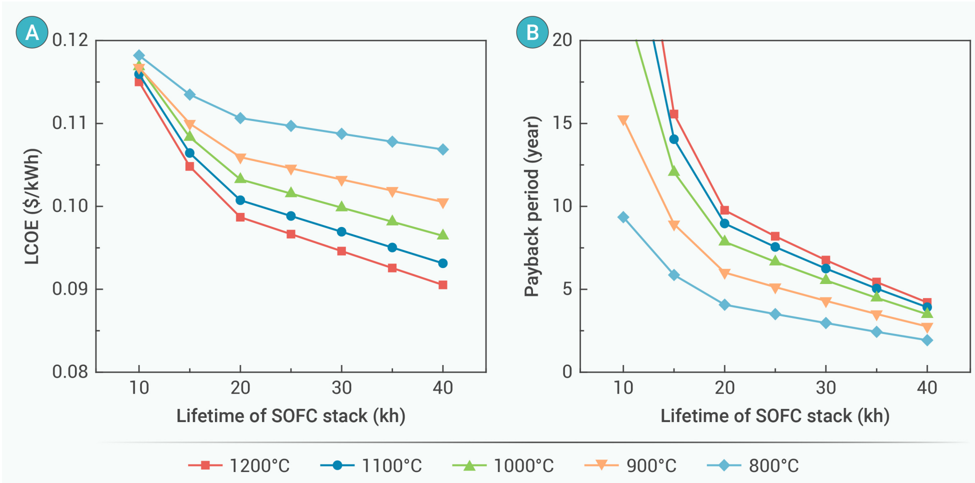

Figure 8. Techno-economic analysis of SOFC-GT hybrid system with different SOFC operating temperature and SOFC stack lifetime (A) LCOE. (B) Payback period.

anode. Moreover, given that steam reforming of hydrocarbons is a strongly endothermic reaction, maintaining elevated temperatures may facilitate the conversion of hydrocarbon fuels into small-molecule gaseous fuels (e.g., CO and H_2), thereby partially alleviating carbon deposition in fuel cells. Finally, fuel pretreatment methods such as external steam reforming or coupling with a catalytic partial oxidation (CPOX) reformer can be employed like conventional SOFCs, while controlling the C/O ratio to prevent carbon deposition. In the Supplemental Information, the carbon deposition of methane has been discussed, and the C/O ratios for steam reforming and CPOX should be kept below 1 as shown in the C-H-O ternary diagram of Figure S2.

(4) Output power scalability. Enhancing power scalability of SHT-SOFCs is essential for industrial-scale deployment, requiring solutions to two key challenges: single-cell power scaling and stack integration. For single-cell scaling, efficient current collection architectures are critical, since the ionic conductivity of the YSZ electrolyte is significantly enhanced, which leads to a low ohmic impedance of only 26 mΩ in this study, while the current collection resistance does not decrease with temperature. As the active area of a single SOFC unit expands, the proportion of current collection resistance within the total cell impedance will rise substantially, which severely limits single-cell power scaling. To address this, we think that the "segmented-in-series" configuration developed by Mitsubishi Heavy Industries (MHI) offers a promising solution for super-high-temperature SOFC unit power scaling,[5] which elevating cell voltage while reducing current to minimize current collector loss. Regarding stack integration, intensified reaction kinetics at super-high temperatures accelerate fuel consumption and heat generation, necessitating optimized geometries and fuel channels to ensure uniform temperature and concentration fields and prevent localized overheating and starvation. Moreover, effective thermal management strategies including excess air cooling and endothermic fuel internal reforming can be applied to balance the extreme heat generation of SHT-SOFCs.

CONCLUSION

In this study, to overcome the efficiency improvement bottleneck of large-scale gas turbine, we proposed a strategy of integrating an SHT-SOFC stack operating above 1200°C with a commercial hundred-MW-class gas turbine featuring a TIT higher above 1400°C. The necessity of elevating the SOFC operating temperature in a hundred-MW-class hybrid system was validated through simulations, thermodynamically analyzed using a T-s indicator diagram in terms of area combination. The main conclusions are as follows:

(1) The concept of SHT-SOFC operating at 1200°C was validated using a tubular SOFC fabricated in our laboratory, which achieved a peak output power of 4.67 W. Compared with a conventional SOFC operating temperature of 700°C, the peak power of the tubular SOFC increased by a factor of 5.5 when the operating temperature was elevated to 1200°C.

(2) In the hundred-MW-hybrid system, when the SOFC operating temperature increases from 800°C to 1200°C, the temperature mismatch between the SOFC and the F-class gas turbine is significantly reduced from 68.16% to 0%. This reduction is accompanied by an increase in FCC exergy efficiency from 76.52% to 85.93%, as well as an increase in system efficiency from 58.60% to 74.12%.

(3) A super-high system efficiency of 80.31% can be expected when the SOFC operating temperature is further elevated to 1300°C.

(4) Extending the SHT-SOFCs lifespan is crucial for improving the techno-economic performance. When the SHT-SOFC achieved a lifespan of 40 kh, the hybrid power system demonstrated a LCOE of 0.0905 $/kWh with an investment payback period of 4.21 years.

In future study, several challenges need to be addressed for large-scale industrial applications, which mainly include durability, power density and multi-fuel compatibility. If these issues can be properly resolved, SHT-SOFCs will not only hold great promise for large-scale stationary power generation applications but could also emerge as a promising candidate for some mobile application such as auxiliary power units (APUs) in large long-endurance aircraft.

REFERENCES

1. Buonomano A., Calise F. and D Accadia M.D., et al. (2015). Hybrid solid oxide fuel cells–gas turbine systems for combined heat and power: A review. *Appl. Energy* **156**:32–85. DOI:10.1016/j.apenergy.2015.06.027
2. Choudhary T. and Sanjay (2017). Thermodynamic assessment of advanced SOFC-blade cooled gas turbine hybrid cycle. *Int. J. Hydrog. Energy* **42**: 10248-10263. DOI: doi.org/10.1016/j.ijhydene.2017.02.178.
3. Pirkandi J. and Ommian M. (2019). Thermo-economic operation analysis of SOFC–GT combined hybrid system for application in power generation systems. *J. Electrochem. Energy Convers. Storage* **16**:11001. DOI: doi.org/10.1115/1.4040056.
4. Yi Y., Smith T.P. and Brouwer J., et al. (2003). Simulation of a 220 kW hybrid SOFC gas turbine system and data comparison. *ECS Proceedings Volumes* **2003-07**:1442–1454. DOI:10.1149/200307.1442PV
5. Kobayashi Y., Ando Y. and Kishizawa H., et al. (2013). Recent progress of SOFC-GT combined system with tubular type cell stack at MHI. *ECS Transactions* **51**:79–86. DOI:10.1149/05101.0079ecst
6. Huang Y. and Turan A. (2019). Fuel sensitivity and parametric optimization of SOFC – GT hybrid system operational characteristics. *Therm. Sci. Eng. Prog.* **14**:100407. DOI:10.1016/j.tsep.2019.100407
7. Eisavi B., Chitsaz A. and Hosseinpour J., et al. (2018). Thermo-environmental and economic comparison of three different arrangements of solid oxide fuel cell-gas turbine (SOFC-GT) hybrid systems. *Energy Conv. Manag.* **168**:343–356. DOI:10.1016/j.enconman.2018.04.088
8. Hajabdollahi Z. and Fu P. (2017). Multi-objective based configuration optimization of SOFC-GT cogeneration plant. *Appl. Therm. Eng.* **112**:549–559. DOI:10.1016/j.applthermaleng.2016.10.103
9. Shamoushaki M., Ehyaei M.A. and Ghanatir F. (2017). Exergy, economic and environmental analysis and multi-objective optimization of a SOFC-GT power plant. *Energy* **134**:515–531. DOI:10.1016/j.energy.2017.06.058
10. Sghaier S.F., Khir T. and Ben Brahim A. (2018). Energetic and exergetic parametric study of a SOFC-GT hybrid power plant. *Int. J. Hydrog. Energy* **43**:3542–3554. DOI:10.1016/j.ijhydene.2017.08.216
11. Zhang S., Liu H. and Liu M., et al. (2017). An efficient integration strategy for a SOFC-GT-SORC combined system with performance simulation and parametric optimization. *Appl. Therm. Eng.* **121**:314–324. DOI:10.1016/j.applthermaleng.2017.04.066
12. Eveloy V., Karunkeyoon W. and Rodgers P., et al. (2016). Energy, exergy and economic analysis of an integrated solid oxide fuel cell – gas turbine – organic Rankine power generation system. *Int. J. Hydrog. Energy* **41**:13843–13858. DOI:10.1016/j.ijhydene.2016.01.146
13. Gogoi T.K., Sarmah P. and Deb Nath D. (2014). Energy and exergy based performance analyses of a solid oxide fuel cell integrated combined cycle power plant. *Energy Conv. Manag.* **86**:507–519. DOI:10.1016/j.enconman.2014.06.006
14. Turja A.I., Khan I.A. and Rahman S., et al. (2024). Machine learning-based multi-objective optimization and thermal assessment of supercritical CO_2 Rankine cycles for gas turbine waste heat recovery. *Energy and AI* **16**:100372. DOI:10.1016/j.egyai.2024.100372
15. Ashraf W.M. and Dua V. (2024). Data Information integrated Neural Network (DINN) algorithm for modelling and interpretation performance analysis for energy systems.

Energy and AI 16:100363. DOI:10.1016/j.egyai.2024.100363
16. Dunn B., Kamath H. and Tarascon J. (2011). Lowering the temperature of solid oxide fuel cells. *Science* 334:928–935. DOI:10.1126/science.1212741
17. Gao Z., Mogni L.V. and Miller E.C., et al. (2016). A perspective on low-temperature solid oxide fuel cells. *Energy Environ. Sci.* 9:1602–1644. DOI:10.1039/C5EE03858H
18. Duan C., Tong J. and Shang M., et al. (2015). Readily processed protonic ceramic fuel cells with high performance at low temperatures. *Science* 349:1321–1326. DOI:10.1126/science.aab3987
19. Shin S.S., Kim J.H. and Bae K.T., et al. (2020). Multiscale structured low-temperature solid oxide fuel cells with 13 W power at 500 °C. *Energy Environ. Sci.* 13:3459–3468. DOI:10.1039/D0EE00870B
20. Gülen S.C. and Zachary J. (2022). Feasibility of achieving 62% combined cycle efficiency with a 200 MW gas turbine. *Proceedings of ASME Turbo Expo* 2022:V005T09A003. DOI: doi.org/10.1115/GT2022-81807.
21. Perna A., Minutillo M. and Jannelli E., et al. (2018). Performance assessment of a hybrid SOFC/MGT cogeneration power plant fed by syngas from a biomass down-draft gasifier. *Appl. Energy* 227:80–91. DOI:10.1016/j.apenergy.2017.08.077
22. Barelli L., Bidini G. and Ottaviano A. (2017). Integration of SOFC/GT hybrid systems in Micro-Grids. *Energy* 118:716–728. DOI:10.1016/j.energy.2016.10.100
23. Koç Y., Yağlı H. and Görgülü A., et al. (2020). Analysing the performance, fuel cost and emission parameters of the 50 MW simple and recuperative gas turbine cycles using natural gas and hydrogen as fuel. *Int. J. Hydrog. Energy* 45:22138–22147. DOI:10.1016/j.ijhydene.2020.05.267
24. Yin F. and Rao A.G. (2020). A review of gas turbine engine with inter-stage turbine burner. *Prog. Aeosp. Sci.* 121:100695. DOI:10.1016/j.paerosci.2020.100695
25. Li J. and Li Y. (2023). Micro gas turbine: Developments, applications, and key technologies on components. *Propuls. Power Res.* 12:1–43. DOI:10.1016/j.jppr.2023.01.002
26. Ghotkar R. and Milcarek R.J. (2020). Investigation of flame-assisted fuel cells integrated with an auxiliary power unit gas turbine. *Energy* 204:117979. DOI:10.1016/j.energy.2020.117979
27. Reyhani H.A., Meratizaman M. and Ebrahimi A., et al. (2016). Thermodynamic and economic optimization of SOFC-GT and its cogeneration opportunities using generated syngas from heavy fuel oil gasification. *Energy* 107:141–164. DOI:10.1016/j.energy.2016.04.010
28. Maghsoudi P. and Sadeghi S. (2020). A novel economic analysis and multi-objective optimization of a 200-kW recuperated micro gas turbine considering cycle thermal efficiency and discounted payback period. *Appl. Therm. Eng.* 166:114644. DOI:10.1016/j.applthermaleng.2019.114644
29. Bao C., Shi Y. and Li C., et al. (2010). Multi-level simulation platform of SOFC–GT hybrid generation system. *Int. J. Hydrog. Energy* 35:2894–2899. DOI:10.1016/j.ijhydene.2009.05.047
30. Bao C., Shi Y. and Croiset E., et al. (2010). A multi-level simulation platform of natural gas internal reforming solid oxide fuel cell–gas turbine hybrid generation system: Part I. *Solid oxide fuel cell model library. J. Power Sources* 195:4871–4892. DOI: doi.org/10.1016/j.jpowsour.2010.01.078.
31. Bao C., Cai N. and Croiset E. (2011). A multi-level simulation platform of natural gas internal reforming solid oxide fuel cell–gas turbine hybrid generation system – Part II. *Balancing units model library and system simulation. J. Power Sources* 196:8424–8434. DOI: doi.org/10.1016/j.jpowsour.2011.05.032.
32. Li Q., Zuo W. and Zhang Y., et al. (2020). Effects of rectangular rib on exergy efficiency of a hydrogen-fueled micro combustor. *Int. J. Hydrog. Energy* 45:10155–10163. DOI:10.1016/j.ijhydene.2020.01.221
33. Udomsilp D., Rechberger J. and Neubauer R., et al. (2020). Metal-supported solid oxide fuel cells with exceptionally high power density for range extender systems. *Cell Rep. Phys. Sci.* 1:100072. DOI:10.1016/j.xcrp.2020.100072
34. Li C., Ning X. and Li C. (2005). Effect of densification processes on the properties of plasma-sprayed YSZ electrolyte coatings for solid oxide fuel cells. *Surface and Coatings Technology* 190:60–64. DOI:10.1016/j.surfcoat.2004.04.086
35. Wang Y., Gao J. and Chen W., et al. (2020). Development of ScSZ electrolyte by very low pressure plasma spraying for high-performance metal-supported SOFCs. *J. Therm. Spray Technol.* 29:223. DOI:10.1007/s11666-019-00970-1
36. Cui T., Li H. and Lyu Z., et al. (2022). Identification of electrode process in large-size solid oxide fuel cell. *Acta Phys.-Chim. Sin.* 38:2011009. DOI: doi.org/10.3866/PKU.WHXB202011009.
37. Chen J., Li Y. and Zhang H., et al. (2021). Comparison of different fuel cell temperature control systems in an anode and cathode ejector-based SOFC-GT hybrid system. *Energy Conv. Manag.* 243:114353. DOI:10.1016/j.enconman.2021.114353
38. Beigzadeh M., Pourfayaz F. and Ghazvini M., et al. (2021). Energy and exergy analyses of solid oxide fuel cell-gas turbine hybrid systems fed by different renewable biofuels: A comparative study. *J. Clean. Prod.* 280:124383. DOI:10.1016/j.jclepro.2020.124383
39. Leal E.M., Bortolaia L.A. and Leal Junior A.M. (2019). Technical analysis of a hybrid solid oxide fuel cell/gas turbine cycle. *Energy Conv. Manag.* 202:112195. DOI:10.1016/j.enconman.2019.112195
40. Ezzat M.F. and Dincer I. (2020). Energy and exergy analyses of a novel ammonia combined power plant operating with gas turbine and solid oxide fuel cell systems. *Energy* 194:116750. DOI:10.1016/j.energy.2019.116750
41. Wang X., Lv X. and Weng Y. (2020). Performance analysis of a biogas-fueled SOFC/GT hybrid system integrated with anode-combustor exhaust gas recirculation loops. *Energy* 197:117213. DOI:10.1016/j.energy.2020.117213
42. Huang Y. and Turan A. (2021). Mechanical equilibrium operation integrated modelling of recuperative solid oxide fuel cell – gas turbine hybrid systems: Design conditions and off-design analysis. *Appl. Energy* 283:116237. DOI:10.1016/j.apenergy.2020.116237
43. Soleymani E., Ghavami Gargari S. and Ghaebi H. (2021). Thermodynamic and thermoeconomic analysis of a novel power and hydrogen cogeneration cycle based on solid SOFC. *Renew. Energy* 177:495–518. DOI:10.1016/j.renene.2021.05.103
44. Lv X., Liu X. and Gu C., et al. (2016). Determination of safe operation zone for an intermediate-temperature solid oxide fuel cell and gas turbine hybrid system. *Energy* 99:91–102. DOI:10.1016/j.energy.2016.01.047
45. Ding X., Lv X. and Weng Y. (2019). Coupling effect of operating parameters on performance of a biogas-fueled solid oxide fuel cell/gas turbine hybrid system. *Appl. Energy* 254:113675. DOI:10.1016/j.apenergy.2019.113675
46. Baranowski M., Bober M. and Kudyba A., et al. (2019). The effect of surface condition on wetting of HASTELLOY® X by brazing filler metal of Ni-Pd-Cr-B-Si system. *J. Mater. Eng. Perform.* 28:3950–3959. DOI:10.1007/s11665-019-03998-0
47. https://www.hpalloy.com/Alloys/descriptions/HASTELLOY_X.aspx.
48. Gamanov S., Holzer J. and Roupcova P., et al. (2022). High temperature oxidation kinetics of Fe-10Al-4Cr-4Y_2O_3 ODS alloy at 1200–1400 °C. *Corros. Sci.* 206:110498. DOI:10.1016/j.corsci.2022.110498
49. Wang Y., Ren J. and Shi Y., et al. (2019). Numerical model of direct internal reforming SOFC: A comparison between anode-support and metal-support. *ECS transactions* 91:2013–2022. DOI:10.1149/09101.2013ecst

FUNDING AND ACKNOWLEDGMENTS

This work was supported by the National Natural Science Foundation of China (52322609), National Natural Science Foundation of China (52394203) and the Fundamental Research Funds for the Central Universities (2023CX01003). The funders had no role in study design, data collection and analysis, decision to publish, or preparation of the manuscript.

DECLARATION OF INTERESTS

The authors declare no competing interests.

DATA AND CODE AVAILABILITY

Data are available from the corresponding author upon reasonable request.

SUPPLEMENTAL INFORMATION

It can be found online at https://doi.org/10.59717/j.xinn-energy.2025.100096

LEAD CONTACT WEBSITE

https://www.te.tsinghua.edu.cn/info/1101/1712.htm